Quantitative Assessment on the Importance of Purity on the Properties of Single Wall Carbon Nanotubes

Naoyuki Matsumoto[†], Guohai Chen[†], Motoo Yumura[†,‡], Don N. Futaba[†,‡,], Kenji Hata[†,‡,*]*

Affiliation

[†] Technology Research Association for Single Wall Carbon Nanotubes (TASC), Central 5, 1-1-1 Higashi, Tsukuba, Ibaraki 305-8565, Japan

[‡] National Institute of Advanced Industrial Science and Technology (AIST), Central 5, 1-1-1 Higashi, Tsukuba, Ibaraki 305-8565, Japan

*Corresponding authors. Tel: +81-29-861-4851. E-mail: d-futaba@aist.go.jp (D. N. Futaba), kenji-hata@aist.go.jp (K. Hata).

Table of contents entry
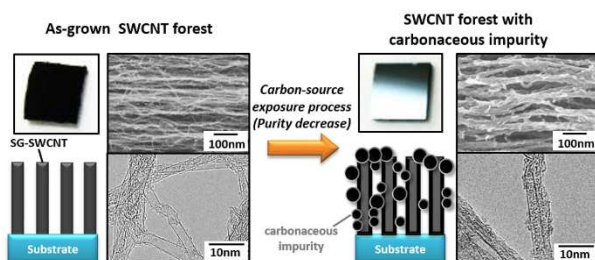
Abstract

We quantitatively demonstrate the importance of high purity on the application of single wall carbon nanotubes (SWCNTs), a material solely composed of a surface, by examining the effects of carbon impurities on the electrical, thermal, and mechanical properties for both the as-grown SWCNT forests and processed buckypaper. While decreases in properties were expected, our results showed the extreme sensitivity of SWCNT properties on carbonaceous impurities either through scattering in the individual SWCNTs or the inhibition in the ability to form inter-SWCNT junctions. Each property showed nonlinear decreases (as high as 40%) with the addition of low levels of carbon impurities (~15 wt%), and which demonstrates that purity is as important as the crystalline structure.

KEYWORDS: Single wall carbon nanotube, carbonaceous impurities, thermal property, electrical property, mechanical property, dispersibility.

Historically through the development of materials, the structure has been one of the primary points of focus for the understanding and optimizing of material properties. For example, crystalline structure significantly affects the plasticity and work hardening properties of metals and alloys.[1,2] However, for the actual macro, micro, and nanoscopic structure, the presence of impurities have also been long known to play a significant role in the application materials. For example, for centuries, pig-iron was known to suffer from sulfur and phosphorous, which increased brittleness and made casting impossible.[3]

Carbon nanotubes (CNTs) are no exception to history. CNTs have been extensively studied due to their unique set of electrical, thermal, mechanical, and optical properties, which stem from their graphitic, pseudo-one dimensional structure.[4-12] As a result, the application of CNTs have been widely explored to realize their potential ranging from super-capacitors, and electric motors and generators, heat exchangers as thermal/electrical conductive polymer (rubber), and metal composites.[13-15] However, CNTs are never free from carbonaceous impurities which are adsorbed on and around the CNT surface and severely affect properties.[16] The effects on application performance has been well documented.[16-27] For example, Vilela *et al.* reported the effects of purity on SWCNTs as demonstrated on the electrochemical sensing performance in SWCNT microfluidic chips where higher purity SWCNT-based electrodes exhibited a 3-fold higher sensitivity, very good signal-to-noise ratio, high resistance-to-fouling, and 2-fold enhancement in resolution.[17] In addition, Kang *et al.* demonstrated a high performance triode amplifier (gate turn-on voltage of 20 V, high anode current of 134 μA, and current density of ~7.0 A/cm^2) by post-synthesis rapid thermal annealing to reduce carbonaceous impurities.[18] Further, Han *et al.* demonstrated a ~28 times decrease (5380 to 187 Ohm/□) in sheet resistance

by multiple purifications of the CNTs.[19] The mechanisms for performance degradation due to impurities on single-walled carbon nanotubes (SWCNTs) has been elucidated, *i.e.* electron scattering which reduced electrical conductivity and phonon scattering and resonance shifting which reduced thermal conductivity.[28,29] As a result, purification processes have been developed; however, the effects also include damage to the SWCNTs through scission. Despite these developments, the quantitative assessment for the effect of carbonaceous impurities on electrical, thermal conduction, and processing *etc.* has not yet been elucidated due to the inability to quantitatively measure the absolute purity. Recently, quantitative and objective methods to evaluate the levels of carbonaceous impurities in macroscopic forms of SWCNTs have been reported. Haddon *et al.* reported a method using Near-IR (NIR) spectroscopy for relative purity estimation .[30] Yasuda *et al.* proposed a method to estimate the absolute purity, that is, the weight fraction of SWCNTs, based on a the exposure to the growth ambient.[16] Futaba *et al.* used outer specific surface area as an analytical method for measuring the absolute purity.[31] Therefore, we understand the effects of carbonaceous impurities and know how to quantify them, but these two important aspects have not been combined to experimentally elucidate the quantitative assessment of the importance of purity on the properties of SWCNTs.

In this report, we quantitatively examined the changes in performance after known levels of carbonaceous impurity deposition on the as-grown SWCNTs, the ability to be dispersed, and the properties as a processed sheet (buckypaper). Our results demonstrated that not only did every property decrease, the profiles for the various declines were similar, characterized by an extreme drop (25-75%) within the first 15% decrease in purity from the near pristine (~100% purity) SWCNTs. Thus, these results demonstrate the need for highly clean SWCNT surfaces, as an increase in 10% increase in purity will result in much more than a 10% increase in property

performance.

Our strategy to quantitatively assess the importance of purity on the properties of SWCNTs, we characterized the family of SWCNTs at various stages: from the as-grown state through the processing to a buckypaper, *i.e.* as a forest, the dispersion, and as a processed form. In this manner, we could characterize the changes to the intrinsic properties of the SWCNTs (*i.e.* forest) at each stage.[32-36]

To begin, a family of identical SWCNT forests were fabricated which differed only in the purity (Fig. 1a). To avoid the effects induced by purification process, we did the reverse and first synthesized high purity SWCNT forests which were identical in every aspect: purity, average diameter (2.8 nm), height (500 μm), and density (0.03 g/cm^3) *etc.* and controllably decreased purity by controlled exposures to the growth ambient (Methods). We had very strict requirements on the starting material. First, we required a SWCNT which did not require any purification in order to avoid the purification damage. Second, we required high SWCNT selectivity. Third, to avoid non-carbonaceous impurity effects, we required SWCNT material with high carbon purity, i.e. negligible levels of catalyst and support materials. Finally, we required the material to consist of a high absolute purity (i.e. SWCNT wt% or little to no carbonaceous impurities) to allow for subsequent control of purity. Forests were ~500 μm in height, and average diameter of the SWCNTs within the forest was ~2.8 nm. While several high purity methods have been reported in the literature. Super-growth chemical vapor deposition (CVD) was chosen because it could meet all of our purity criteria.[37-40] This method has been shown to synthesize highly purity, catalyst-free SWCNTs, with an outer specific surface area of 1150 m^2/g (ideal: 1315 m^2/g), which corresponded to SWCNTs with an absolute purity of ~97% (*i.e.* ~3% carbonaceous impurities) in an aligned and self-assembled structure.[31] Therefore, our starting material

approached the condition of nearly ideally clean SWCNTs without the need for any potentially

damaging post-synthetic processes. Each forest in this set was then removed from the catalyst

substrate and subjected to different exposures of carbon feedstock (ethylene) to create a family of

SWCNT forests differing only by purity ranging from 97 to 35%. Specifically, we defined the

"absolute impurity" as the weight change before and after ethylene exposures as following

equation (1):

$$Absolute\ Purity\ (\%) = 100 \times [m_{SWNT} / (\Delta G + m_{SWNT})]\ (1)$$

where ΔG is the weight of impurities, and m_{SWNT} is the initial weight of the SWNT forest,

respectively. [16]

Our first observation of as-grown SWCNT forests with high purity (97%) were

exceptionally black, consistent with previous reports of SWCNTs acting as nearly perfect

absorbers (Fig. 1a).[41] As the purity decreased, the color of the forests appeared more grey-black

with slight metallic luster (~40%), and appeared silver-grey with an appearance of graphite

(~35%) (Fig. 1a). Similar to previous reports of carbonaceous impurities, the impurities adsorbed

on and between the SWCNTs, as a coating and agglomerates.[16,31] As the amount of carbonaceous

impurities increased, the Raman spectra showed a decrease in the graphitic to disorder band ratio

(Raman G- to D-band ratio) and a gradual disappearance of the Raman radial breathing modes

(RBM). Further, the macroscopic forest density exhibited a nearly three-fold increase with

decreasing purity from 0.035 g/cm^3 at 97% purity to 0.10 g/cm^3 at 35% purity (Fig. 1c inset). In

addition, as the purity decreased, the pore size distribution, which was estimated by the Barrett-

Joyner-Halenda (BJH) method from nitrogen adsorption isotherms, showed a monotonic

decrease (Supplemental Fig. S1).[42]
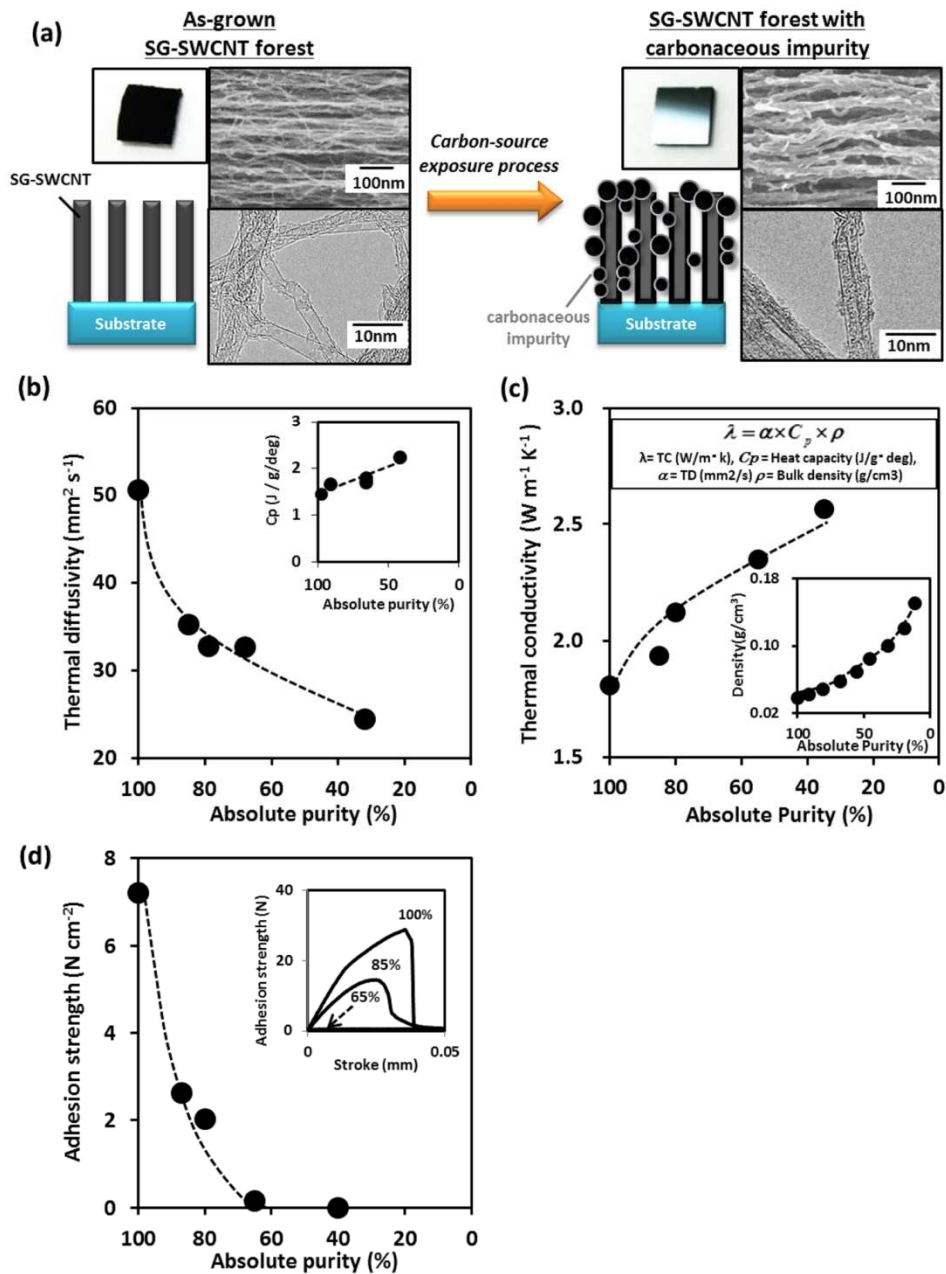
Fig. 1 Schematic, scanning electron microscope, and transmission electron microscope images, with inset digital photographs of the (a) as-grown and ~60% purity SWCNTs. Plots of the (b) thermal diffusivity as a function of absolute purity (inset: plot of specific heat vs absolute purity). (c) Plot of the thermal conductivity as a function of absolute purity (inset: plot of macroscopic forest density vs absolute purity). (d) Plot of the dry adhesive strength of the SWCNT forests as a function of absolute purity (inset: Stress-strain plots for three purities).

Thermal diffusivity and conductivity, and dry adhesion of the SWCNT forests showed exceptional sensitivity to the presence of carbonaceous impurities characterized by an initially nonlinear drop followed by plateauing (Fig. 1 b-d). While not a perfect model for an individual SWCNTs, the SWCNT forests provided a unique analog to investigate the effect on the individual CNTs because each SWCNT spans the vertical height of the forest. The thermal diffusivity along the alignment direction was measured using the flash method for the family of forests and plotted as a function of absolute purity.[43] The thermal diffusivity response to a decrease in purity was characterized by a sharp 45% decrease from 50.5 mm^2/s at 97 % to 27.6 mm^2/s at ~60 %, which was followed by a gradual plateauing at 24.3 mm^2/s at ~35% purity (Fig. 1b). The observed rapid decrease in thermal diffusivity demonstrates the extreme sensitivity of the SWCNTs to the presence of carbonaceous impurities stemming from both damping and scattering at the impurity adsorption sites.[44] The correspondence between this behavior and the suppression of the Raman RBM signatures is direct evidence that the decrease in thermal diffusivity stems from damping and scattering as they pertain to coherent phonon propagation.[45] The thermal conductivity was estimated from the density and specific heat for each sample and plotted as a function of the absolute purity (Fig. 1c). While the thermal conductivity increased ~40% from 1.81 to 2.56 W/(m・K) across our purity range, this resulted from the ~3 times increase in macroscopic forest density as described above.

To examine the effects of carbon impurities on the mechanical aspects of SWCNTs, the dry adhesive strength in the normal direction to a glass contact surface was investigated. The similarity of the CNT to the gecko spatula has shown strong dry adhesive properties on glass surfaces.[46] The adhesive pull-off strength for each member in the family of forests was measured and plotted as a function of absolute purity (Fig. 1d). The adhesive strength dropped nonlinearly,

most sharply within the first ~15% decrease in purity, yet with several differences. First, the adhesion strength dropped more significantly, ~70%, from 7.20 to 2.03 N/cm^2, within the first 20% of purity decrease. Second, below a purity of ~60%, the forest failed to exhibit any measurable adhesion. These results are also observable in the stress-strain curves for three purity levels (Fig. 1d, inset). The observed decrease in the dry adhesion strength of the SWCNT forests vividly demonstrates how even the smallest presence of impurities can inhibit the ability for the SWCNTs to form long and intimate contacts, which are required for strong adhesion (*i.e.* strain transfer).[46] This point was further supported by the absence of SWCNTs on the counter surface after failure, which indicated the weak SWCNTs to glass adhesion strength. It is interesting to note that our results show that SWCNT forests possessing ~90% purity, which would be generally regarded as high purity and have a specific surface area of 1100 m^2/g, showed less than half the adhesive strength compared to the ideal levels. These results taken together illustrate the significant detrimental effects of even small levels of carbonaceous impurities (< 15%) on the properties of the individual SWCNTs. These results highlight the importance of purity, and that even a small increase in purity can lead to a significant payoff in property performance.

As the dispersion of SWCNTs represents a vital route from the raw material to a processed form, the effect of purity on the dispersion was very important for SWCNT applications. Our results showed that the increased presence of carbonaceous impurities adversely affected the dispersibility of SWCNTs. The family of SWCNTs was dispersed in methyl isobutyl ketone (MIBK). MIKB was used as it is a common solvent for composite manufacture.[47] The ability to disperse was quantified as the concentration of SWCNTs in the dispersed solution as calculated based on Lambert-Beer's Law from UV-vis absorbance of the supernatant solution.[48]
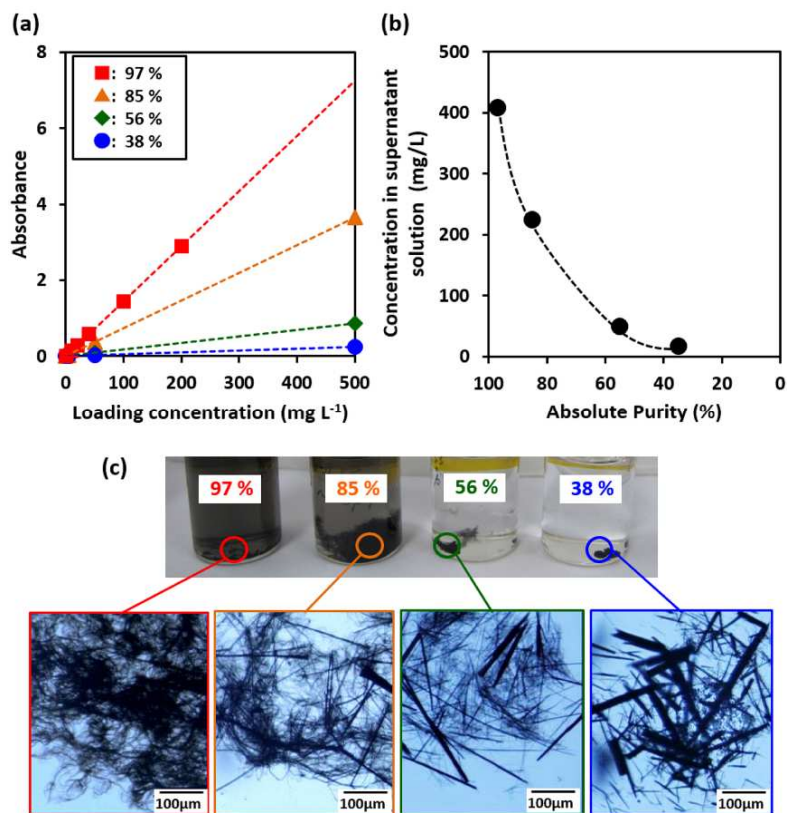
Fig. 2 (a) Plot of the absorbance as a function of loading concentration for different purity SWCNTs. (b) Calculated dispersed concentration as a function of absolute purity. (c) Digital photographs for several dispersed SWCNTs of different purities and for undispersed fraction.

The absorbance spectra was measured for each dispersion and plotted as a function of purity. The absorbance of the supernatant solution decreased as the purity decreased (*i.e.* increased carbonaceous impurity) (Fig. 2a), which indicated that content of dispersed SWCNTs diminished as the carbonaceous impurities increased. The ability to disperse the SWCNTs dropped ~87% from 400 mg/L at high purity 97% to less than 50 mg/L at relatively low purity, ~55% (Fig. 2b). In addition, the dispersion homogeneity decreased (Fig. 2c). For SWCNTs of 97% purity, the dispersion was uniformly black with a small amount of undispersed SWCNTs visible in the bottle and visibly lightened for decreased purity (Fig. 2c). While previous reports

have indicated the improvement of SWCNT dispersibility due to the presence of carbonaceous impurities, our results suggest that debundling of the SWCNTs plays a more significant role.[48] Microscope images of the nondispersed SWCNTs show that the level of debundling significantly decreased for forests with lower purity (Fig. 2c). Nondispersed fraction for the high purity (97%) and lower purity (35%) appeared as highly randomly oriented 3-D network and needles, respectively (Fig. 2c). We believe that the dispersion with Bahr *et al.* is more of a result of the different materials, ~500 μm long, ~2.8 nm SWCNTs in MIBK compared with ~500 nm long, *c.a.* 0.7 nm SWCNTs in 1,2-dichlorobenzene.[48] We expect that with the presence of impurities results in a dimensionality change from the pseudo-one dimensional SWCNTs to spherical as well as a thermodynamic change in surface energy to play roles.[49] Our results indicate that the primary obstacle in dispersion is the reduction in exfoliation.

To quantify the impact of carbonaceous impurities on a macroscopic assembly, the family of SWCNT forests was processed into a family of SWCNT buckypapers varying only by the purity. Structurally, in contrast to vertically aligned forests where individual SWCNTs vertically span, the buckypaper structure is as an assembly of interconnected SWCNTs. Thusly, unlike the properties of SWCNT forests reflect the individual SWCNTs, those of the buckypaper are governed by both the individual SWCNTs and by the intertube junctions. As such, this examination of a macroscopic assembly provides further insight into the quantitative assessment to clarify the importance of purity on the properties of SWCNTs. The buckypapers (φ36) were identically fabricated, and the electrical conductivity, thermal diffusivity and conductivity, and mechanical breaking strength were characterized. The buckypapers showed obvious color and density variations, where those made from high purity SWCNTs (purity: ~97%) appeared black (Fig 3a, inset) and possessed high density (~0.32 g/cm^3), and buckypapers made from lower

purity SWCNTs (purity: 38%) appeared increasingly grey-black, possessing one-quarter the density (~0.075 g/cm^3) (Fig. 3a, 3c, inset). The gradual decrease in density is indicative of the gradual adsorption of carbonaceous impurities into the SWCNT materials which hinders the efficient packing.[16] The effect of density on electrical and thermal conductivities is well known, but it is worth noting that the density could not be maintained for all purities.
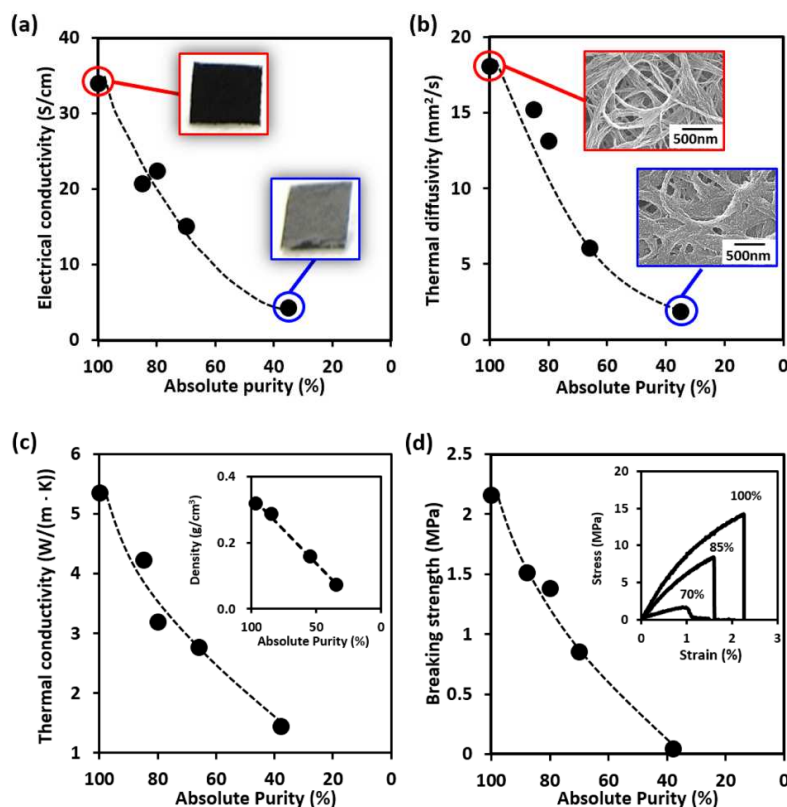

Figure 3: Buckypaper property characterization. (a) Plot of the electrical conductivity as a function of the absolute purity (inset: digital photograph of the buckypapers of different purities). (b) Thermal diffusivity as a function of the absolute purity (inset: scanning electron microscope images of buckypapers of different purities). (c) Thermal conductivity as a function of the absolute purity (inset: macroscopic density of buckypaper vs absolute purity). (d) Breaking strength as a function of the absolute purity (inset: stress-strain profiles for three buckypapers of different purities).

When each buckypaper was characterized and the results plotted as a function of absolute purity, the dependences of the electrical conductivity, thermal diffusivity and conductivity, and mechanical breaking strength were similar, characterized by an initially nonlinear drop followed by plateauing (Fig. 3). Electrical conductivity of the fabricated buckypapers, as measured by the four probe method, showed a monotonic decrease which included an asymptotic approach to 15% as that of the high purity buckypaper. In fact, the electrical conductivity decreased ~40% with a ~15% purity drop (from 34.0 to 20.7 S/cm) (Fig. 3a). The thermal diffusivity and thermal conductivity exhibited strong dependence on presence of carbon impurities. The in-plane thermal diffusivity (along the plane of the CNTs), measured in air at room temperature by a thermo-wave analyzer showed a similar non-linear, monotonic, and asymptotic decrease from 18.1 mm^2/s at 97 % purity to 13.1 mm^2/s at 80% purity (Fig. 3b). Similarly, the thermal conductivity, as calculated from the thermal diffusivity, specific heat, and density, exhibited a 75% decrease from ~5.4 to 1.4 W/(m・K) (Fig. 3c). Interestingly, when comparing the thermal diffusivity vs. purity profiles between the buckypapers and forests, the initial severe decrease of 40% for the first 15% decrease in purity was nearly identical, which would imply a similar decline mechanism, *i.e.* phonon damping and scattering from impurity adsorption of the individual SWCNTs. Below ~15% purity, the thermal diffusivity of the buckypaper continued its steep decrease and approached zero unlike results for the SWCNT forests. Although more fundamental study is required to clarify this difference, we believe this behavior stems from poor phonon transfer through CNT-impurity-CNT junctions. Finally, examination of the buckypaper mechanical breaking strength was carried out by measuring the stress-strain failure response of dog-boned shaped buckypapers by a static mechanical analyzer (Fig. 3d). The breaking strengths of the buckypaper decreased sharply on the level of carbonaceous impurities, and decreased until

nearly zero breaking strength was observed at ~35% purity. Stress-strain responses further illustrate the differences in buckypaper cohesiveness, where both Young's modulus and breaking strain decreased rapidly with increased carbon impurity (Fig. 3d, inset). This is experimentally supported by the presence of large quantities of CNT (and bundles) emanating from the fractured surface. For the buckypaper, the electrical, thermal, and mechanical properties, when combined with those from dry adhesion, further support the detrimental effects of impurities on the ability of the SWCNTs to form intimate inter-tube junctions, which are required for efficient electron, phonon, and strain transfer. This phenomenon is similar to the observed enhanced electrochemical sensing performance of microfluidic chips with purified, rather than unpurified, SWCNTs.[17]

In conclusion, we have quantitatively investigated the impact of carbonaceous impurities on the properties of SWCNTs, the ability to disperse, and their properties as an assembled form (buckypaper) by varying only the purity and not the structure, such as crystallinity and length. While our results may not represent the ideal or highest reported values, our results quantitatively demonstrate the detrimental effects of carbon impurities on the SWCNTs, a material solely composed of a surface, at most stages of processing, which has never been previously reported. Furthermore, as the synthetic structural control further advances, these results demonstrate that purity is as important as crystallinity, length, and diameter, on property improvement and should not be neglected as low purity could easily offset high crystallinity using SWCNTs. Conversely, the strong and immediate effect of carbonaceous impurity presented in this report demonstrate that the improvement in properties for increased purity are well worth the effort as even a 15% increase in purity would provide a 270% increase in forest adhesion, 180% increase in dispersibility, and 170% increase in buckypaper electrical

conductivity. Therefore, purity management (< 85%) at all levels of synthesis, lab-scale to industrial-scale, is important to utilize the unique and advantageous properties of SWCNTs.

Experimental Methods

SWCNT forests preparation

SWCNT forests were synthesized in a 1-inch tube reactor from Al_2O_3 (40 nm)/Fe (1.8 nm) catalysts sputtered on silicon wafers with ethylene (100 sccm) and water (~100-200 ppm) using He with H_2 as carrier gases at a total flow of 1 liter per minute at 750 °C. The forest consists of aligned SWCNTs (~2.8nm) with high selectivity (99% single wall) and was very sparse (mass density: ~0.04 g/cm^3).[50] The outer specific surface area (SSA) estimated by using the t-plot formulation from N_2 adsorption-desorption isotherms with a BEL Japan BELSORP Mini II surface-area and pore-size analysis system.[31]

Purity Reduction Process

The purity of the forests was controllably reduced from the as-grown level by removing it from the substrate and then exposure to different amounts of carbon feedstock (ethylene) at 750 °C similar to previous reports.[16, 31] Because the starting, as-grown material possessed a high absolute purity, the purity following carbon deposition was calculated directly from the weight gain from to this exposure process.[16] We note that because the forests were removed from the catalyst substrate and that the amount of residual catalyst material is negligible, and the contribution of additional CNT growth to the weight could be neglected.

Property characterization

The thermal diffusivity of the forests along the alignment direction was measured using the flash method with a Xe-lamp source (NETZSCH, LFA 447 Nano Flash). The specific heat was estimated by differential scanning calorimetry (DSC, Hitachi High-Tech Science Corporation, EXSTAR X-DSC7000). The normal mechanical adhesion was characterized using a static mechanical analyzer (Shimadzu, MST-I) with a preload of 180 N/cm^2 onto a glass contact surface.

The ability to disperse was quantified as the concentration of SWCNTs in the dispersed solution, which was determined from UV-vis absorbance and concentration of the supernatant solution based on Lambert-Beer's Law. First, measurement of known concentrations to make an adsorption-concentration plot is needed to determine the attenuation coefficient of the dispersion by the following relationship, $A = \varepsilon l c$, where ε is the attenuation coefficient, l is the optical path length, c is the concentration, and A is the absorbance. [47] The attenuation coefficient at 500 nm by this method was determined to be 2.06 x 10^4 cmg^{-1}. Determination of the concentration of each of our samples was then performed by dispersing 1 mg of SWCNTs in MIBK by high pressure jet-milling at 60 MPa (JOKOH, JN-5) and ultrasonication at 200W for 30 min (SHARP, UT-206). The solutions were left to settle for 3 hrs, and the absorption spectra of the dispersion were measured using a UV-vis spectrophotometer (UV-3600, Shimadzu). The dispersion concentrations were then estimated using the above relationship with the attenuation now known.

The buckypapers were fabricated by vacuum filtration of the dispersed CNTs in MIBK and left to dry at 180 $^\circ$C for 5 h, and the electrical, thermal, and mechanical properties were characterized as previous report.[36] Electrical conductivity was calculated from the measured sheet resistance

using a commercial four probe electrical measurement tester (Mitsubishi chemical, Loresta-EP MCP-T360) and the average cross-sectional height.[36] Thermal diffusivity (in plane) was measured at room temperature in air by a thermowave analyzer (TA3, Bethel Co., Ltd). Mechanical breaking strength was estimated by measuring the stress-strain failure response of dog-boned shaped buckypapers by a static mechanical analyzer (Shimadzu, MST-I).

Notes

Acknowledgements

References

1. E. Ma, T. D. Shen and X. L. Wu, *Nat. Mater.,* 2006, **5**,515–516.

2. Z. Wang, M. Saito, K. P. McKenna and Y. Ikuhara, *Nat. Comm.*, 2014, **5**, 3239–1–8.

3. H. Thompson, Engineers and Engineering (Past-into-present), B.T. Batsford Ltd., London, 1976.

4. S. P. Frank, P. Poncharal, Z. L. Wang and W. A.de Heer, *Science*, 1998, **280**, 1744–

1746.

5.   W. J. Liang, M. Bockrath, D. Bozovic, J. H. Hafner, M. Tinkham and H. Park, *Nature*, 2001, **411**,665–669.

6.   R. H. Baughman, A. A. Zakhidov and W. A. de Heer, *Science*, 2002, **297**, 787–792.

7.   P. Kim, L. Shi, A. Majumdar and P. L. McEuen, *Phys. Rev. Lett.*, 2001, **87**, 215502.

8.   M. Kociak, A. Y. Kasumov, S. Guéron, B. Reulet, I. I. Khodos, Y. B. Gorbatov, V. T. Volkov, L. Vaccarini and H. Bouchiat, *Phys. Rev. Lett.*, 2001, **86**, 2416–2419.

9.   Z. K. Tang, L. Zhang, N. Wang, X. X. Zhang, G. H. Wen, G. D. Li, J. N. Wang, C. T. Chan and P. Sheng, *Science*, 2001,**292**, 2462–2465.

10. E. W. Wong, P. E. Sheehan and C. M .Lieber, *Science*, 1997, **277**, 1971–1975.

11. D. A. Walters, L. M. Ericson, M. J. Casavant, J. Liu, D. T. Colbert, K. A. Smith and R. E. Smalley, *Appl. Phys. Lett.*, 1999, **74**, 3803–3805.

12. M.-F. Yu, B. S. Files, S. Arepalli and R. S. Ruoff, *Phys. Rev. Lett.*, 2000, **84**, 5552–5555.

13. C. M. Niu, E. K. Sichel, R. Hoch, D. Moy and H. Tennent, *Appl. Phys.Lett.*, 1997, **70**, 1480–1482.

14. H. Zhidong and F. Alberto, *Progress in Polymer Sci.*, 2011, **36**, 914–944.

15. K. Fukuchi, K. Sasaki, K. Katagiri, T. Imanishi and A Kakitsuji, *Procedia Eng.*, 2011, **10**, 912–917.

16. S. Yasuda, T. Hiraoka, D. N. Futaba, T. Yamada, M. Yumura and K. Hata, *Nano Lett.*, 2009, **9**, 2585–2590.

17. D. Vilela, A. Anson-Casaos, M. T. Martinez, M. C. Gonzaleza and A. Escarpa, *Lab Chip*, 2012, **12**, 2006–2014.

18. Y. M. Wong, W. P. Kang, J. L. Davidson and J. H. Huang, *Diamond Relat. Mater.*, 2007,

16, 1403–1407

19. J. Y. Woo, D. Kim, J. Kim, J. Park and C. S. Han, *J. Phys. Chem. C*, 2010, **114**, 19169–19174.

20. S. II Jung, S. H. Jo, H. S. Moon, J. M. Kim, D. S. Zang and C. J. Lee, *J. Phys. Chem. C*, 2007, **111**, 4175–4179.

21. W. Huang, Y. Wang, G. Luo and F. Wei, *Carbon*, 2003, **41**, 2585–2590.

22. I. Y. Y. Bu, K. Hou and D, Engstrom, *Diamond Relat. Mater.*, 2011, **20**, 746–751.

23. I. W. Chiang, B. E. Brinson, R. E. Smalley, J. L. Margrave and R. H. Hauge, *J. Phys. Chem. B*, 2001, **105**, 1157–1161.

24. S. K. Choi and S. B. Lee, *Current Appl. Phy.*, 2009, **9**, 658–662.

25. D. K. Singh, P. K. Iyer and P. K. Gir, *J. Appl. Phy.*, 2010, **108**, 084313.

26. M. K. Seo and S. J. Park, *J. Korean Phys. Soc.*, 2009, **55**, 656–660.

27. E. Minoux, O. Groening, K. B. K. Teo, S. H. Dalal, L. Gangloff, J. P. Schnell, L. Hudanski, I. Y. Y. Bu, P. Vincent, P. Legagneux, G. A. J. Amaratunga and W. I. Milne, *Nano Lett.*, 2005, **5**, 2135–2138.

28. P. R. Bandaru, *J. Nanosci. Nanotech.*, 2007, **7**, 1–29.

29. J. Hone, M. Whitney, C. Piskoti and A. Zettl, *J. Phys. Chem. B*, 1999, **59**, R2514–2516.

30. A. Yu, E. Bekyarova, M. E. Itkis, D. Fakhrutdinov, R. Webster and R. C. Haddon, *J. Am. Chem. Soc.*, 2006, **128**, 9902–9908.

31. D. N. Futaba, J. Goto, T. Yamada, S. Yasuda, M. Yumura and K. Hata, *Carbon*, 2010, **48**, 4542–4546.

32. H. Liu, Y. Feng, T. Tanaka, Y. Urabe and H. Kataura, *J. Phys. Chem. C*, 2010, **114**, 9270–9276.

33. K. Kordás, T. Mustonen, G. Tóth, H. Jantunen, M. Lajunen, C. Soldano, S. Talapatra, S. Kar, R. Vajtai and P. M. Ajayan, *Small*, 2006, **2**, 1021–1025.

34. K. Kobashi, S. Ata, T. Yamada, D. N. Futaba, M. Yumura and K. Hata, *Chem. Sci.*, 2013, **4**, 727–733

35. T. Sekitani, Y Noguchi, K. Hata, T. Fukushima, T. Aida and T. Someya, *Science,* 2008, **321**, 1468–1472.

36. S. Sakurai, F. Kamada, D. N Futaba, M. Yumura, and K. Hata, *Nanoscale Res. Lett.*, 2013, **8**, 546–1–7.

37. H. Kimura, J. Goto, S. Yasuda, S. Sakurai, M. Yumura, D. N. Futaba and K. Hata, *J. Am. Chem. Soc.*, 2013, **7**, 3150–3157.

38. Z. Chen, D. Y. Kim, K. Hasegawa and S. Noda, *ACS nano*, 2013, **7**, 6719–6728.

39. T. Chen, M. Zhao, Q. Zhang, G. Tian, J. Huang and Fei Wei, *Adv. Funct. Mater.*, 2013, **23**, 5066–5073.

40. C. Paukner and K. K. K. Koziol, *Sci. Rep.*, 2014, **4**, 3903.

41. K. Mizuno, J. Ishii, H. Kishida, Y. Hayamizu, S. Yasuda, Don N. Futaba, M. Yumura and K. Hata, *Proceedings National Acade. Sci.*, 2009, **106**, 6044–6047.

42. E. P. Barrett, L. G. Joyner and P. P. Halenda, *J. Am.Chem. Soc* ., 1951, **73**, 373–380.

43. M. Akoshima, K. Hata, Don N. Futaba, K. Mizuno, T. Baba and M. Yumura, *Jpn. J. App. Phy.*, **48**, 2009, 05EC07.

44. K. Hess, *Appl. Phys. Lett.*, 1979, **35**, 484−486.

45. C. Thomsen and S. Reich, *Topics Appl. Phy.*, 2007, **108**, 115–232.

46. L. Qu, L. Dai, M. Stone, Z. Xia and Z. L. Wang, *Science*, 2008, **322**, 238−242.

47. H. Yoon, M. Yamashita, S. Ata, D. N. Futaba, T. Yamada and K. Hata, *Sci. Rep.*, 2014,

4, 3907.

48. J. L. Bahr, E.T. Mickelson, M. J. Bronikowski, R. E. Smalley and J. M. Tour, *Chem. Comm.*, 2001, 193–194.

49. S. D. Bergin, V. Nicolosi, P. V. Streich, S. Giordani, Z. Sun, A. H. Windle, P. Ryan, N. P. P. Niraj, Z. T. Wang, L. Carpenter, W. J. Blau, J. J. Boland, J. P. Hamilton and J. N. Coleman, *Adv. Mater.*, 2008, **20**, 1876–1881.

50. K. Hata, D. N. Futaba, K. Mizuno, T. Namai, M. Yumura and S. Iijima, *Science* 2004, **306**, 1362–1364.